



Elevated $p\text{CO}_2$ Level Affects the Extracellular Polymer Metabolism of *Phaeodactylum tricornutum*

Wei Zhang¹, Xuexi Tang^{1,2*}, Yingying Yang¹, Xin Zhang¹ and Xinxin Zhang^{1,2*}

¹ Department of Marine Ecology, College of Marine Life Sciences, Ocean University of China, Qingdao, China, ² Laboratory for Marine Ecology and Environmental Science, Qingdao National Laboratory of Oceanology for Marine Science and Technology, Qingdao, China

OPEN ACCESS

Edited by:

Ondrej Prasil,
Academy of Sciences of the Czech
Republic, Czechia

Reviewed by:

Graham J. C. Underwood,
University of Essex, United Kingdom
Bernard Lepetit,
University of Konstanz, Germany

*Correspondence:

Xuexi Tang
tangxx@ouc.edu.cn
Xinxin Zhang
zhangxinxin@ouc.edu.cn

Specialty section:

This article was submitted to
Aquatic Microbiology,
a section of the journal
Frontiers in Microbiology

Received: 07 November 2019

Accepted: 17 February 2020

Published: 04 March 2020

Citation:

Zhang W, Tang X, Yang Y, Zhang X
and Zhang X (2020) Elevated $p\text{CO}_2$
Level Affects the Extracellular Polymer
Metabolism of *Phaeodactylum*
tricornutum. *Front. Microbiol.* 11:339.
doi: 10.3389/fmicb.2020.00339

Extracellular polymeric substances (EPS) play an important role in diatom physiology and carbon biogeochemical cycling in marine ecosystems. Both the composition and yield of EPS in diatom cells can vary with environmental changes. However, information on intracellular pathways and controls of both biochemical and genetic of EPS is limited. Further, how such changes would affect their critical ecological roles in marine systems is also unclear. Here, we evaluated the physiological characteristics, EPS yields, EPS compositions, and gene expression levels of *Phaeodactylum tricornutum* under elevated $p\text{CO}_2$ levels. Genes and pathways related to EPS metabolism in *P. tricornutum* were identified. Carbohydrate yields in different EPS fractions increased with elevated $p\text{CO}_2$ exposure. Although the proportions of monosaccharide sugars among total sugars did not change, higher abundances of uronic acid were observed under high $p\text{CO}_2$ conditions, suggesting the alterations of EPS composition. Elevated $p\text{CO}_2$ increased PSII light energy conversion efficiency and carbon sequestration efficiency. The up-regulation of most genes involved in carbon fixation pathways led to increased growth and EPS release. RNA-Seq analysis revealed a number of genes and divergent alleles related to EPS production that were up-regulated by elevated $p\text{CO}_2$ levels. Nucleotide diphosphate (NDP)-sugar activation and accelerated glycosylation could be responsible for more EPS responding to environmental signals. Further, NDP-sugar transporters exhibited increased expression levels, suggesting roles in EPS over-production. Overall, these results provide critical data for understanding the mechanisms of EPS production in diatoms and evaluating the metabolic plasticity of these organisms in response to environmental changes.

Keywords: extracellular polymeric substances, *Phaeodactylum tricornutum*, elevated $p\text{CO}_2$, adaptation, metabolic plasticity, RNA-seq

INTRODUCTION

Extracellular polymeric substances (EPS) produced by microorganisms primarily comprise acid mucopolysaccharides (Mcconville et al., 1985), are ubiquitous in aquatic environments (Sutherland, 1999; Donot et al., 2012), and play important roles in cellular adhesion, signaling, and stress responses (Underwood and Paterson, 2003; Taylor et al., 2013). Diatoms are one of the most

abundant photosynthetic organisms in oceans where they occupy diverse habitats and are one of the primary contributors of EPS pools in marine ecosystems. Polysaccharide-rich EPS released by diatoms can be utilized as a carbon source by bacteria, meiofauna, and macrofauna (Middelburg et al., 2000). Indeed, diatom EPS is an important component of marine dissolved organic matter (DOM) (Deming, 2010; Underwood et al., 2013) and is thus an integral component of the oceanic carbon cycle in addition to other cycles (Simon et al., 2002). Moreover, the formation of micro-environments by diatom EPS promotes microbial interactions within and around EPS matrices (Sonnenschein et al., 2011).

Extracellular polymeric substances are considered important adaptations of diatoms to their environments. For example, they can play an important role in the stability of intertidal flats and the formation of sediments (de Brouwer et al., 2005, 2002). Further, EPS form buffer zones between cells and environments, thereby helping diatom cells withstand low temperatures, desiccation, salinity stress, and toxicant exposure (Aslam et al., 2012; Steele et al., 2014). Concomitantly, EPS has the potential to interact with various ions or compounds via an abundance of polar functional groups, and can thereby alter the bioavailability and toxicity of compounds (Czaczyk and Myszk, 2007). The composition and structure of EPS varies in response to the growth environments of diatoms (Abdullahi et al., 2006; Ai et al., 2015). For example, algae respond to inorganic nutrient constraints, salinity, and low temperature stress by altering their EPS production rates as well as their chemical properties (Underwood et al., 2004; Abdullahi et al., 2006; Mishra and Jha, 2009). Moreover, studies have shown that the monosaccharide components, protein contents, molecular weights, and surface properties of EPS may affect their activities and counteract external interference (Calazans et al., 2000; Song et al., 2015).

During EPS synthesis, monosaccharides are converted to NDP-sugars by multiple pathways and then assembled into polysaccharides. This mechanism of production is evolutionarily conserved among prokaryotes and eukaryotes. The polysaccharides are further incorporated into EPS in the Golgi apparatus and then transported via vesicles to cellular membranes and excreted (Gügi et al., 2015; Aslam et al., 2018). Complex genetic networks are necessary to enable cells to flexibly respond to their environments by altering EPS characteristics (Underwood et al., 2004; Aslam et al., 2018). A recent study identified the metabolic pathways for EPS production in the polar diatom *Fragilariopsis cylindrus* that changed in response to temperature and salinity gradients, suggesting that their metabolic plasticity was attributable to molecular complexity (Aslam et al., 2018). However, it is unclear if these responses are characteristic of only psychrophilic algae like *F. cylindrus* or are instead common features of diatom taxa in other environments.

Increasing CO₂ concentrations alters the chemical nature of seawater carbonates as well as the availability and toxicity of nutrients (Millero et al., 2009). Marine organisms such as phytoplankton, mussels, and fish are particularly sensitive to changes in carbonate chemistry, and elevated pCO₂ levels could have profound effects on marine ecosystems (Doney et al., 2009). Thus, the possible biological consequences of elevated

pCO₂ levels has recently received extensive research attention. In particular, several studies have reported the effects of elevated pCO₂ levels on diatoms at the physiological and ecological scales (Wu et al., 2010; Gao and Campbell, 2014; Shi et al., 2019). However, few studies have evaluated the molecular mechanisms underlying diatom responses to elevated pCO₂ levels. Indeed, many mechanisms by which diatoms adapt and respond to elevated pCO₂ levels remain unknown.

Despite that EPS plays important roles in the responses of diatoms to environmental changes, variation in diatom EPS in response to elevated pCO₂ levels is unknown. Further, the commonalities of EPS synthesis and mechanisms of metabolism have not been clarified among different diatom taxa from different environments. Given the above lack of information, the response of EPS characteristics to elevated pCO₂ levels in addition to the EPS metabolic pathways of *Phaeodactylum tricornutum* were investigated in the present study. *P. tricornutum* is a model species for diatom biology with clear genetic background, unique evolutionary status and properties that can be routinely transformed (Scala et al., 2002; Kooistra et al., 2003). Further, the genetic background of *P. tricornutum* has been described in detail and was thus leveraged to investigate the effects of elevated pCO₂ levels on the organism. *P. tricornutum* was cultured under different pCO₂ levels for approximately 200 generations, and several parameters were investigated among treatments including changes in growth characteristics, morphology, photophysiology, and the differences in carbohydrate yields within EPS. Metabolic pathways for EPS production were also evaluated in context of the algal response to elevated pCO₂ levels. The results of this study provide important baseline data to develop an understanding of the regulation of key genes involved in the metabolic plasticity of diatoms in response to environmental signals.

MATERIALS AND METHODS

Algal Cultures and the Elevated pCO₂ Experimental System

The *P. tricornutum* (Bacillariophyta, Pennatae, NPECC640) culture was obtained from the Algal Center of the Institute of Oceanology of the Chinese Academy of Sciences. The cells were cultured in modified *f/2* medium (Guillard, 1975) at 20 ± 1°C, with illumination at 120 μmol photon m⁻² s⁻¹ under 12 h light:12 h dark cycles. Flasks were shaken twice a day at fixed times. Cells in the mid-logarithmic growth phase were used for assays. All experiments were conducted in triplicate in 500 mL sterilized and acid-washed Erlenmeyer flasks containing 350 mL of medium. The equipment used in this study was similar to that used in previous investigations (Hutchins et al., 2007; Wu et al., 2010; Fu et al., 2012; Jin et al., 2015). Prior to inoculation, the media were infused with different pCO₂ concentrations. The low CO₂ treatment media was bubbled with ambient air (400 ppmv, LC, pH_{NBS} 8.16), while the high CO₂ treatment media was bubbled with pre-mixed air-CO₂ mixtures (1,000 ppmv, HC, pH_{NBS} 7.82) using a plant growth CO₂ chamber (HP400G-D, Ruihua Instrument & Equipment, Ltd., Wuhan,

China), controlling the CO₂ concentration with a less than 3% variation. Triplicates of LC and HC cultures were all started with the same initial cell densities of 1×10^4 cells mL⁻¹. Every 24 h, a portion of the culture was removed and the remaining culture has refreshed with *p*CO₂ and a pH adjusting medium to maintain the desired pH and *p*CO₂ values within a range of less than 0.5%. Semi-continuous cultivation was used to maintain pH stability over the *P. tricornutum* growth period (Jin et al., 2015). The cultures were grown semi-continuously and were pre-acclimated to experimental conditions for more than 30 generations. Cultures were harvested after 200 generations of semi-continuous incubation. Significant differences were observed in the carbonate systems among different cultures (Supplementary Table S1).

Cell Growth Measurements and Morphological Observations

Cell densities were measured using a particle count and size analyzer (Z2 Coulter, Beckman). The specific growth rate was calculated as follows: $\mu = (\ln N_1 - \ln N_0) \times (t_1 - t_0)^{-1}$, where μ (d⁻¹) is the specific growth rate, and N_0 and N_1 are the cell numbers at times t_0 and t_1 , respectively. After filtering 10 mL of the culture, algal cells were collected and dehydrated, followed by spraying with gold, and placing on a scanning microscope to observe cell morphology. The scanning electron microscope (SEM; model XL-30, Phillips, Eindhoven, Netherlands) was operated at 2.0 kV to observe EPS and cell characteristics.

Determination of Photophysiology

Methanol was used as a solvent to extract pigments from *P. tricornutum* (Macías-Sánchez et al., 2007). Chlorophyll-*a* (Chl *a*) concentrations were determined spectrophotometrically as follows: $\text{Chl } a = 16.29 \times (\text{A}_{665} - \text{A}_{750}) - 8.54 \times (\text{A}_{652} - \text{A}_{750})$, where A₆₅₂, A₆₆₅, and A₇₅₀ represent the absorbances of the methanol extracts at 665, 652, and 750 nm, respectively (Porra et al., 1989). As we did not use the Jeffrey and Humphrey equation (1975) which also corrects for chlorophyll-*c* present in diatoms, these values can only be taken as a proxy for the amount of chlorophyll-*a*. The maximum quantum yields (F_v/F_m) were measured with a Xenon-Pulse Amplitude Modulated Fluorometer (Water-PAM fluorometer, Walz, Effeltrich, Germany) at the middle of the light period of growth. Before the determination, algal cells were dark acclimated for 15 min to obtain completely oxidative PSII reaction centers. Measurement of photosynthetically driven carbon fixation in addition to dark respiration were conducted as described previously (Wu et al., 2010; Hong et al., 2017).

Extraction of Carbohydrate Fractions and Compositional Analysis

Based on previously established sequential extraction methods (Abdullahi et al., 2006), 50 mL of algal culture was used to fractionate the diatom EPS into: (I) a soluble (colloidal) fraction containing both colloidal carbohydrate extractions (CL) a polymeric fraction (cEPS fraction); (II) a hot water (HW)-extracted carbohydrate fraction mainly consisting of

intracellular storage polysaccharides; (III) a hot bicarbonate (HB)-extracted fraction (relative to gelatinous and water-insoluble extracellular polysaccharides) and (IV) a hot alkali extraction (HA) liberating EPS associated with the silica frustules. The concentrations of carbohydrates in each fraction were determined using a phenol sulfuric acid assay, a uronic acid assay with a standard carbazole assay, and neutral monosaccharide compositions were determined by gas chromatography coupled to mass spectrometry. Monosaccharide compositions within carbohydrate fractions were compared using ANOSIM and SIMPER statistical tests (Primer v.6, Plymouth, United Kingdom).

RNA Extraction, Library Preparation, and Illumina Sequencing

Phaeodactylum tricornutum cells in the middle of the light period from three biological replicates were harvested after 200 generations of semi-continuous incubation using vacuum filtration on 1.2 μm polycarbonate filters (Millipore, United States), quickly frozen in liquid nitrogen and maintained at -80°C until use. Total RNA was extracted from frozen cell pellets using the TRIzol[®] Reagent (Invitrogen, Carlsbad, CA, United States) according to the manufacturer's instructions, and DNase (Sigma-Aldrich, St. Louis, MO, United States) was added to digest the DNA. RNA integrity was evaluated using an Agilent 2100 Bioanalyzer (Agilent Technologies, Santa Clara, CA, United States). Extracts with RNA Integrity Number (RIN) ≥ 7 were used for subsequent sequencing library preparation (Supplementary Figure S2). The libraries were constructed using the TruSeq Stranded mRNA LTSample Prep Kit (Illumina, San Diego, CA, United States) according to the manufacturer's instructions. The libraries were then sequenced on the Illumina sequencing platform (HiSeq[™] 2500) by generating 150 bp paired-end reads.

RNA-seq Data Assembly and Analysis

Transcriptomic sequencing and analyses were conducted by OE Biotech, Co., Ltd. (Shanghai, China). Raw data were quality filtered using Trimmomatic v.0.36 (Bolger et al., 2014). Specifically, reads containing poly-N bases and low-quality reads (quality values < 19 accounting for more than 15.0% of the total bases) were removed to obtain clean reads. The reference genome of *P. tricornutum* was downloaded and used for read-mapping¹. Clean reads were mapped to the reference genome using hisat2 (Kim et al., 2015). The Fragments Per Kilobase Million (FPKM) value for each gene was calculated using cufflinks (Trapnell et al., 2010), and the read counts of each gene were obtained by htseq-count (Anders et al., 2015). Differentially expressed genes (DEGs) were then identified using the DESeq (Anders and Huber, 2012) R package functions 'estimate size factors' and 'nbinomTest.' Genes with fold change ratio (HC/LC) ≥ 2 ($P_{\text{adj}} \leq 0.05$) and fold change ratio ≤ 0.5 ($P_{\text{adj}} \leq 0.05$) were defined as "up-regulated genes" and "down-regulated genes," respectively. Hierarchical cluster analysis of DEGs was used to explore patterns of gene expression. Principal component

¹http://protists.ensembl.org/Phaeodactylum_tricornutum/Info/Index

analysis (PCA) and heat map of correlation analysis were then performed based on differences in gene expression levels to investigate overall differences in samples, evaluate inter-sample relationships, and validate experimental designs.

Identification and Hierarchical Clustering Analysis of Carbohydrate Metabolism-Related Proteins

Carbohydrate active enzymes (CAZys) were identified and annotated based on comparisons to the CAZy database² and then clustered with hierarchical clustering using their FPKM values. A one minus Pearson's correlation distance metric and the average linking method was applied to cluster genes and results visualized using the Bioconductor R ComplexHeatmap package (Gu et al., 2016).

Reconstruction of EPS Production Pathways

Extracellular polymeric substances contains abundant polysaccharides and glycans that are assembled and modified within the inner membrane system. The genes involved in the synthesis and metabolism of sugars as well as those involved in EPS assembly and Golgi modification were retrieved from the *P. tricornutum* genome based on comparison against annotations in the GO, KEGG, KOG, and CAZy databases. In addition, hidden Markov models and Hmsearch-3.2.1 (Mitchell et al., 2018) were used to identify nucleotide glycosyltransferases with the nucleotide-sugar transporter (PF04142) model in the *P. tricornutum* genome. Nucleotide glycosyltransferases transport NDP- sugars from the cytoplasm to the Golgi apparatus. Thus, all metabolic genes that were identified were surveyed for the presence of signal peptides using SignalP (Nielsen, 2017). Those proteins that were predicted to be cytosolic, endoplasmic reticulum (ER) associated, or Golgi enzymes that also lacked any conserved plastids (ASAF) or mitochondrial target sequences, were selected for further analysis.

Reverse Transcription Quantitative Real-Time PCR

Reverse transcription quantitative PCR (RT-qPCR) was used to validate the transcriptomic data using primers listed in **Supplementary Table S3**. Polyadenylated RNA was converted to cDNA with the PrimeScript™ II Reverse Transcriptase (TaKaRa, Tokyo, Japan). The RT products were then used as template for qPCR. qPCR reactions were performed on an FTC2000 instrument (Funglyn Biotech, Inc., Toronto, ON, Canada) using SYBR Green I mix (TaKaRa, Tokyo, Japan) in 96-well plates according to the manufacturer's recommendations. The TATA box binding protein and ribosomal protein small subunit 30S (RPS) housekeeping genes (Siaut et al., 2007) were used as references to calibrate expression data. Three biological replicates were conducted for each qPCR reaction.

²www.cazy.org

Data Analysis

All data are expressed as the mean ± SE ($n = 3$). Statistical differences were analyzed by one-way ANOVA tests performed with the SPSS software program (version 22.0) followed by a Tukey's multiple comparisons adjustment, with statistical significance set at $P < 0.05$. All data were tested for normality with Kolmogorov–Smirnov tests and homogeneity of variance with Levene's tests. Redundancy analysis (RDA) was performed using the 'vegan' R package (Oksanen et al., 2003) to identify statistically significant relationships between physiological, biochemical, and transcriptomic datasets. The RDA results were visualized using the ggplot2 R package (Wickham, 2016). Detailed analytical protocols are provided in the **Supplementary Information**. The RNA-seq data were deposited in the ArrayExpress database³ under accession number E-MTAB-8351. Supplementary materials can be found at <https://issues.pangaea.de/browse/PDI-22044>.

RESULTS

P. tricornutum Growth, Morphology, and Photophysiology Under Different pCO₂ Treatments

An increase in the specific growth rate (2.4%) was observed for populations in the HC condition (**Table 1**). F_v/F_m values were higher for the HC condition cells, but significant differences were not observed in pigment contents of cells in the HC and LC treatments. The photosynthetically driven carbon fixation rate and the respiration rate significantly increased (ANOVA, $P < 0.05$) by 13.5% and 33.6% in the HC treatment, respectively. SEM indicated that the preferential morphotype of *P. tricornutum* in both treatments was triradiate (**Figure 1**), which accounted for more than 70.0% of the cellular morphotypes. Morphotype differences were not observed between the LC and HC conditions, but more loosely adhered mucilage occurred near the cells in the HC treatment.

Variation in the Yield and Chemical Composition of Carbohydrates

Compared with the LC treatment, significant increases in carbohydrate yields (ANOVA, $P < 0.05$) were observed for each carbohydrate fraction of *P. tricornutum* in the HC treatment (**Figure 2A**). The CL carbohydrate fraction increased by 31.8% in the HC condition, while the cEPS, HW, HB, and HA fractions increased by 28.4, 34.2, 14.1, and 15.9%, respectively. In particular, the HC treatment conditions stimulated the production of uronic acid in *P. tricornutum*. Compared against the LC conditions, the uronic acid content of the CL, HW, and HB fractions increased significantly in the HC conditions by 1.31-, 1.13-, and 1.41-fold, respectively (**Figure 2B**). Monosaccharide analysis indicated that mannose was the most abundant monosaccharide component of the CL, cEPS, and HA fractions. In contrast, HW fractions were enriched in

³www.ebi.ac.uk/arrayexpress

TABLE 1 | The physiological characteristics of *P. tricornutum* after 200 generations of semi-continuous incubation under LC and HC conditions.

Treatment	μ (d ⁻¹)	Chl a (pg cell ⁻¹)	F_v/F_m	Photosynthetic carbon fixation [μ mol C (μ g chl a) ⁻¹ h ⁻¹]	Dark respiration [μ mol O ₂ (μ g chl a) ⁻¹ h ⁻¹]
LC	1.22 ± 0.01 ^a	0.22 ± 0.01	0.59 ± 0.01 ^a	0.37 ± 0.02 ^a	0.098 ± 0.007 ^a
HC	1.25 ± 0.01 ^b	0.24 ± 0.02	0.62 ± 0.01 ^b	0.42 ± 0.01 ^b	0.131 ± 0.010 ^b

μ , specific growth, Chl a, Chlorophyll-a, and F_v/F_m , maximum quantum yield. The values are means ± SE, and different superscript letters indicate statistically significant differences between LC and HC conditions.

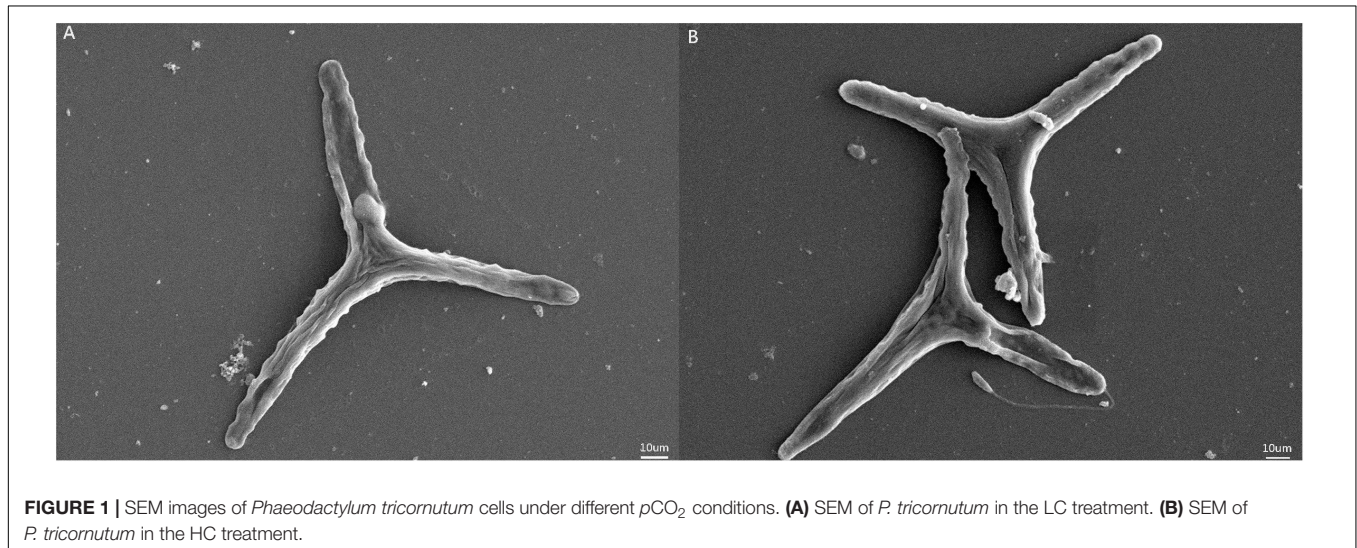


FIGURE 1 | SEM images of *Phaeodactylum tricornutum* cells under different p CO₂ conditions. **(A)** SEM of *P. tricornutum* in the LC treatment. **(B)** SEM of *P. tricornutum* in the HC treatment.

glucose, with glucose generally exceeding 50.0% of the total monosaccharides of those fractions. Galactose was the second most abundant monosaccharide after glucose within the HB carbohydrate fractions. The relative abundances of fucose, arabinose, and rhamnose were lower than those of other monosaccharides. The concentrations of each monosaccharide increased in the HC treatments, while the proportion of monosaccharides of the total sugar content did not significantly change between treatments (Figure 2C).

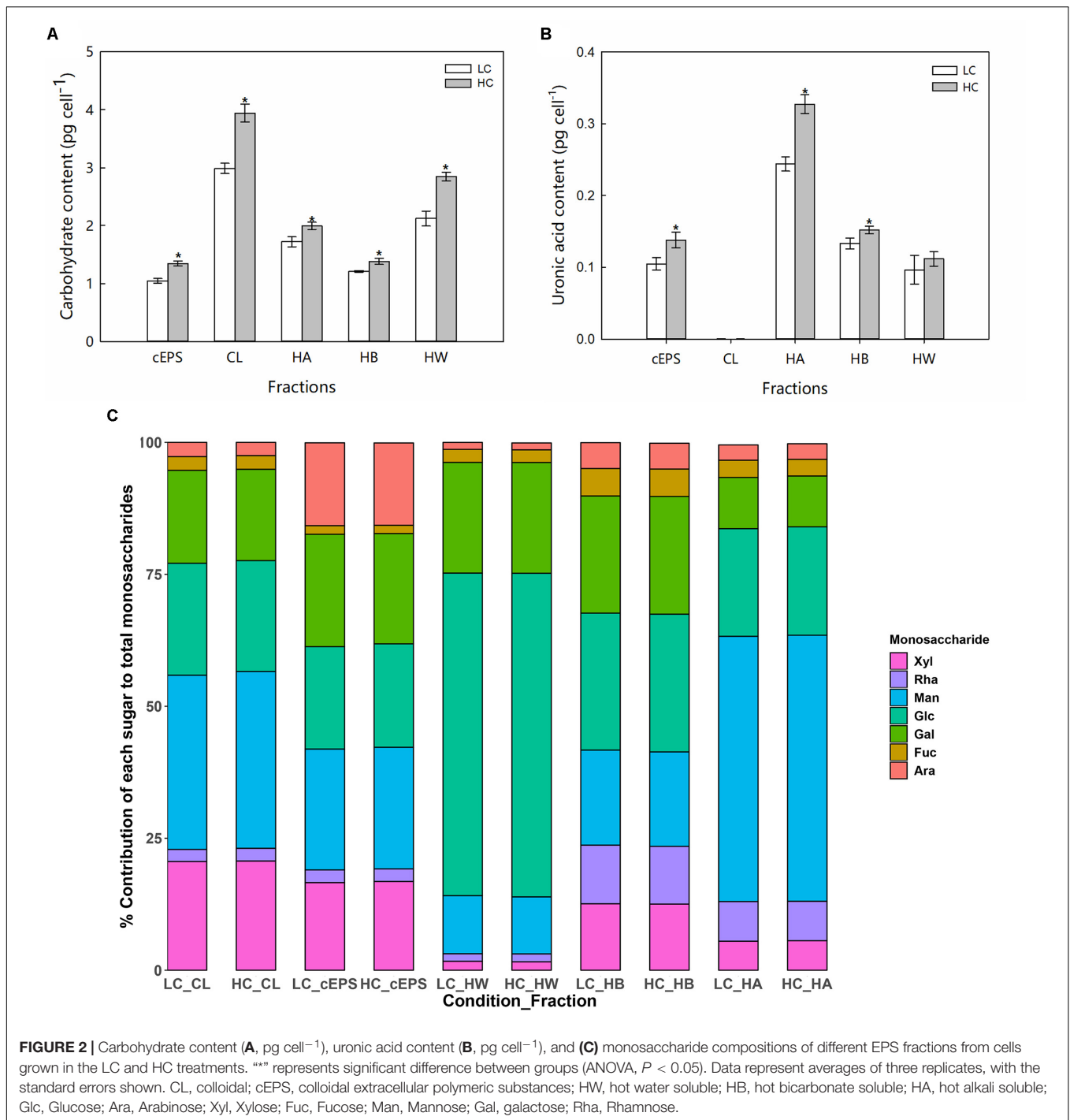
The *P. tricornutum* Transcriptomic Response to High p CO₂ Conditions

RNA-seq data generated from the HC and LC treatment cells were assembled and mapped to the *P. tricornutum* genome. The sequencing analysis of six samples yielded a total of 38.59 Gbp of clean data, with an average of 6.43 Gbp of data per sample. Q30 bases comprised 93.6% of the clean read data and gene coverage was 98.9% or higher. The average total mapping rate of RNA-seq data was about 90.1% (Supplementary Table S2). Thus, the data was of high quality and appropriate for evaluating gene expression in response to HC conditions. Principal component analysis (PCA) of differences in gene expression levels revealed a clear distinction between the two conditions (Figure 3A). The difference between the HC group and the LC group is mainly in the PC1 dimension, which indicates that the difference between the two groups is huge and greatly exceeds the difference within the group. The correlation coefficients among the samples within

groups were 1 (Figure 3B), suggested a good correlation. A total of 2,106 protein coding genes were differentially expressed in the HC condition with 990 up-regulated genes and 1,116 down-regulated genes compared to cells in the LC condition. The up-regulated genes were significantly associated with carbon metabolism (ko01200), carbon fixation in photosynthetic organisms (ko00710), fructose and mannose metabolism (ko00051), Glycolysis/Gluconeogenesis(ko00010) and amino sugar and NDP-sugar metabolism (ko00520), among other pathways (Figure 4A). Down-regulated genes were significantly associated with ribosome biogenesis in eukaryotes (ko03008), RNA transport (ko03013), and spliceosome (ko03040), among other pathways (Figure 4B). Compared with LC condition, genes involved in carbon and fatty acid metabolism are up-regulated, while those involving protein synthesis are down-regulated in HC condition. A high level of concordance was observed between the transcriptomic and RT-qPCR data, thus validating the robustness of the sequencing data (Supplementary Table S3).

Identification of Genes Involved in the Production of EPS

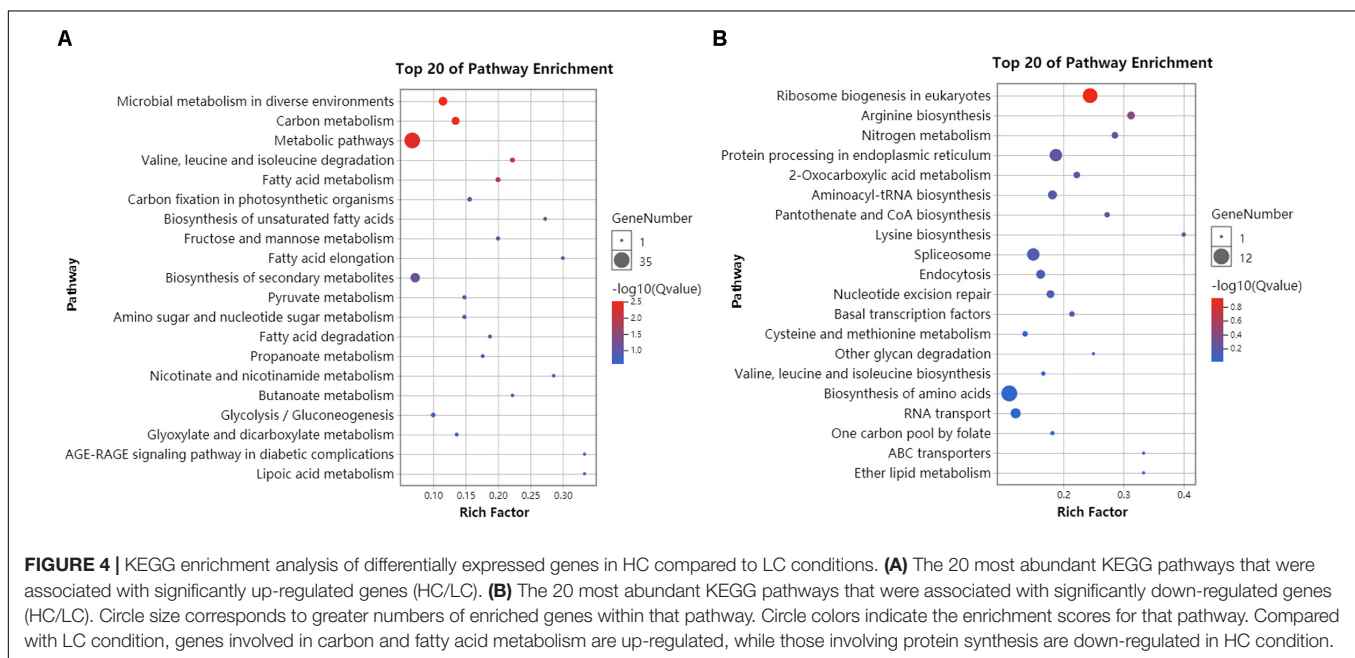
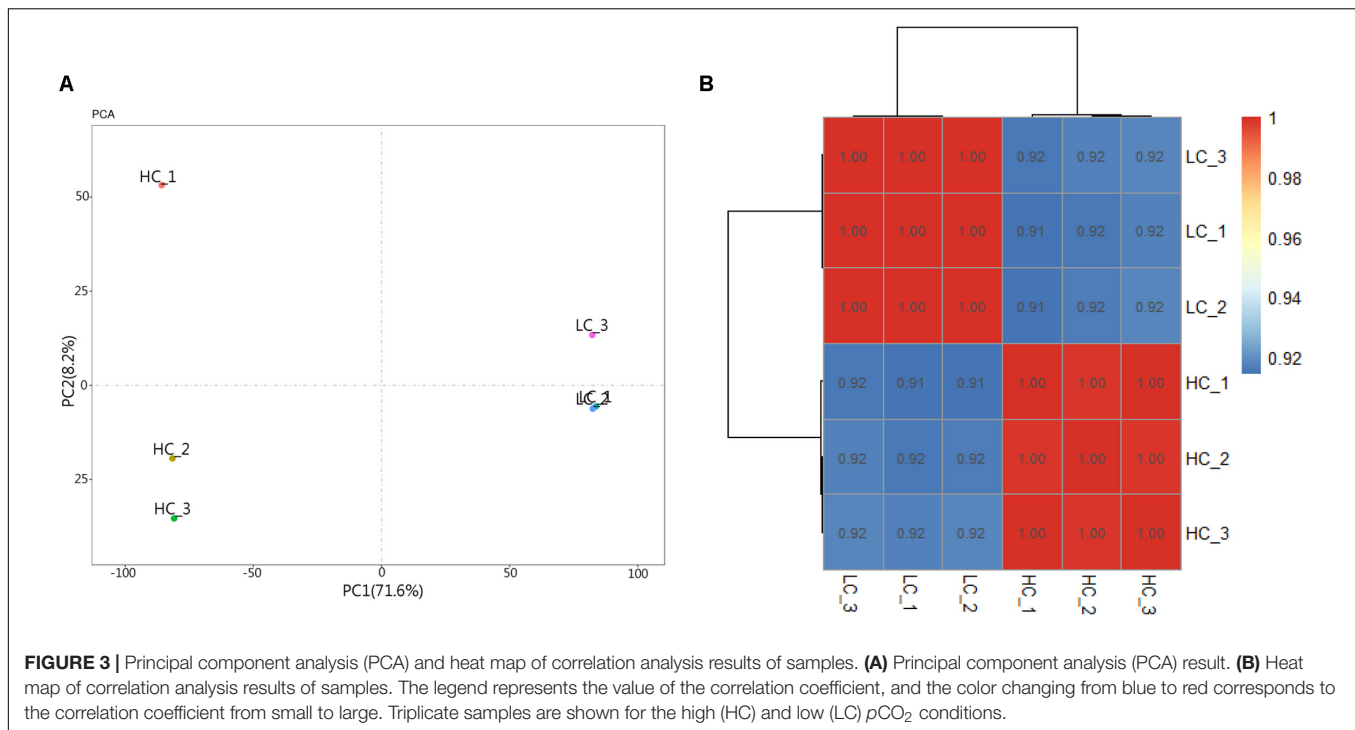
A total of 269 genes encoding carbohydrate active enzymes (CAZy) were identified in the genome including 53 glycoside hydrolases (GHs), 161 glycosyltransferases (GTs), 36 carbohydrate esterases (GEs), and 20 carbohydrate binding modules (CBMs). Four genes (Phatr3_J35856, Phatr3_J48916, Phatr3_J50429, Phatr3_Jdraft1777) encoding carbohydrate active



enzymes were not detected in the expression for both treatment conditions. Cluster analysis of the CAZy protein expression data are shown in **Supplementary Figure S1**, after removal of genes not detected in both treatment conditions. The CAZy proteins could be divided into three clusters based on expression patterns, with 64 down-regulated genes in the first cluster, eight genes with expressions that did not vary between treatments in the second cluster, and the remaining genes belonging to

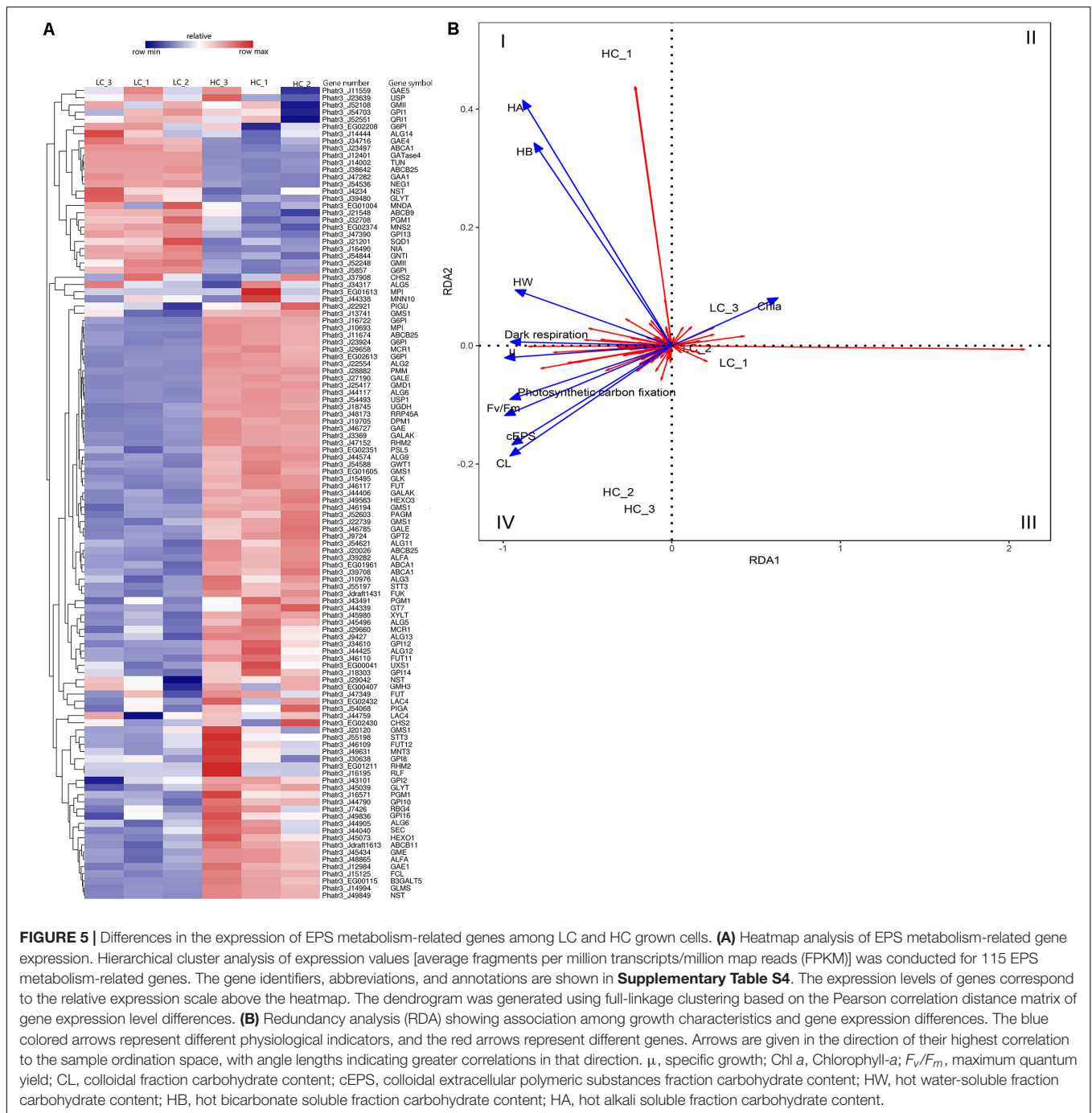
the third cluster. The HC treatment resulted in up-regulation of 72.8% of the genes encoding CAZys. In addition, eight genes encoding nucleotide-sugar transporters were identified by Hmsearch, with seven up-regulated. Phatr3_EG01605 was the most significantly up-regulated gene and encoded a NDP-sugar transporter.

Cluster analysis was conducted using the differences in expression data for 115 protein-coding genes related to



EPS metabolism, including divergent allelic gene copies involved in synthesis pathways of NDP-sugars, NDP-sugar transporters, and glycan synthesis (Figure 5A). Many of the proteins were encoded by more than one gene, including for example, glucose-6-phosphate isomerase and UDP-Glucose-Pyrophosphorylase. Most of the genes involved in NDP-sugars synthesis was up-regulated. Phatr3_EG02613, Phatr3_J10693, Phatr3_J47152, and Phatr3_J25417 were the most significantly up-regulated genes and encoded

phosphoglucumutase, mannose-6-phosphate isomerase, UDP-glucose 4,6-dehydratase, and GDP-mannose 4,6-dehydratase, respectively. These enzymes are important for glucose and mannose activation into NDP-sugars (Figure 6). GDP-mannose can be directly used as a substrate in the endoplasmic reticulum and undergoes modification by several mannosyltransferase (beta-1,4-mannosyltransferase, alpha-1,3/alpha-1,6-mannosyltransferase, alpha-1,3-mannosyltransferase, alpha-1,2-mannosyltransferase,

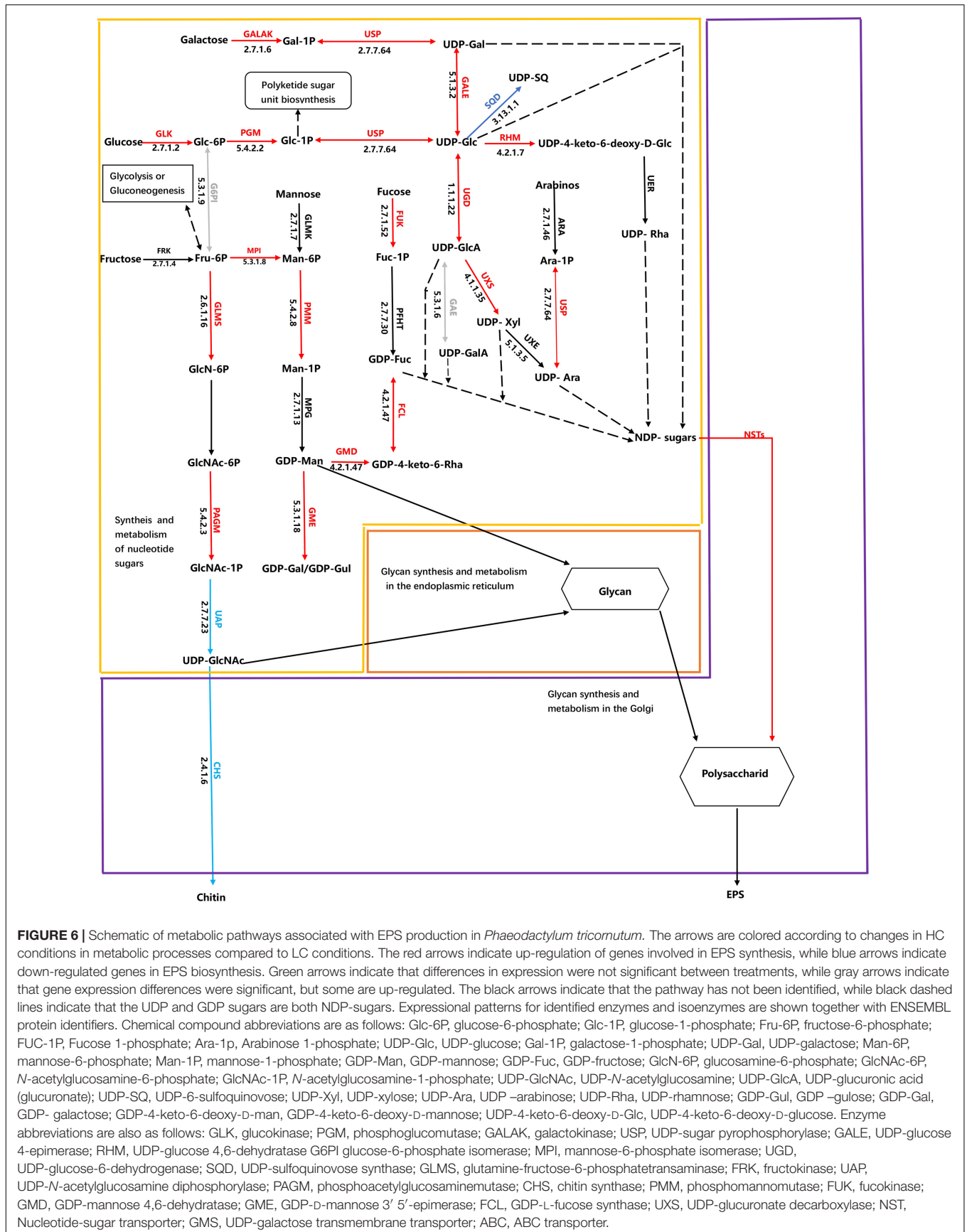


alpha-1,2-mannosyltransferase, etc.), before being assembled into polysaccharides. Other NDP-sugars are transported by NDP-sugar transferases to the Golgi apparatus as substrates, assembled, and then modified into polysaccharides or glycans. In addition, the polysaccharides in the endoplasmic reticulum also enter the Golgi apparatus for further assembly and processing. Most of the genes involved in the assembly and modification of EPS in the Golgi apparatus were up-regulated, although Phatr3_J34317 and Phatr3_J54844 were significantly down-regulated. These genes encode dolichol phosphate

glucosyltransferase and alpha-1,3-mannosyl-glycoprotein-2-beta-*N*-acetylglucosaminyltransferase, respectively.

Relationship Between Gene Expression and the Physiological Status of Diatoms

Positive correlations were observed between diatom growth rate, F_v/F_m values, the photosynthetic carbon fixation rate, and the dark respiration rate, and they were all positively correlated with EPS yield (Figure 5B). The expression levels of Phatr3_J47152



(encoding UDP-glucose 4,6-dehydratase), Phatr3_J25417 (encoding GDP-mannose 4,6-dehydratase), and Phatr3_J27190 (encoding UDP-glucose 4-epimerase) were significantly and positively correlated with diatom growth rate, F_v/F_m , the photosynthetic carbon fixation rate, the dark respiration rate, CL products, and cEPS products. RDA results showed that genes within quadrant one (I) were positively correlated with carbohydrate production of HA, HB, HW, and also positively correlated with dark respiration. The genes in quadrants two and three (II and III) were positively correlated with Chl *a* content. Lastly, the genes in quadrant four (IV) were positively correlated with diatom growth rate, F_v/F_m , photosynthetic carbon fixation rate, and dark respiration rate, in addition to being positively correlated with carbohydrate yields of cEPS and CL.

DISCUSSION

Roles of EPS Released by Diatoms in Response to Environmental Changes

Diatoms produce diverse EPS compounds that vary in structure and sugar composition depending on environmental conditions. The present study reports the first investigation of elevated $p\text{CO}_2$ conditions on EPS released by diatoms. The carbohydrate yields of several EPS fractions (CL, cEPS, HA, and HB) were significantly higher under high CO₂ (HC) conditions. Monosaccharide compositions influence the functional properties of exopolysaccharides, and ultimately determine the rheological properties of EPS, like gel formation (Decho and Gutierrez, 2017). To evaluate the effects of HC conditions on EPS structures, the relative abundances of neutral sugar monosaccharides were determined in the CL-, cEPS-, HB-, and HA-polymers after HC treatment. Complex monosaccharide profiles were clearly observed in the aforementioned EPS fractions produced by *P. tricornutum* (Figure 2C), consistent with previous results (Abdullahi et al., 2006). Compared with the LC treatment cells, there was no significant difference observed in the relative proportions of monosaccharides among the total sugar contents in the HC treatments. In addition, total uronic acid content, which are polymer substituents that also influence physical characteristics, differed considerably between the LC and HC treatments, with increased ionic (uronic) groups observed in algal cells in the HC treatment. Polysaccharides with high proportions of uronic acid often contain an abundance of negatively charged ions and exhibit more available binding sites, leading to greater intra- and inter-chain associations within the polymer or with neighboring polymer groups (Magaletti et al., 2004; Kaplan, 2013). Thus, these results preliminarily suggested that elevated $p\text{CO}_2$ conditions significantly increased EPS production in *P. tricornutum* cells and altered their functional properties.

The secretion of highly complex EPS may function to produce protective cell coatings due to carbohydrate-rich polymers undergoing reversible phase transitions from soluble forms into hydrated forms, followed by condensation into gels in response to environmental changes in ion concentrations, pH, and

temperatures (Decho and Luoma, 1994). For example, the sea-ice diatom *F. cylindrus* reduced growth, but increased yields of EPS under incrementally colder conditions, while an association between EPS, freezing, and cell survival was also observed (Aslam et al., 2012). These observations coincide with the significant increases in polymers observed in this study in response to HC conditions. In addition, microscopic observations (Figure 1) revealed thicker mucilage coatings around *P. tricornutum* cells in the HC treatments. The excess production of EPS has been previously suggested to be due to unbalanced metabolism, wherein carbon-rich polysaccharides are released from cells because of excessive photosynthetic production beyond what is necessary for growth and maintenance of homeostasis (Berman-Frank and Dubinsky, 1999; Hessen and Anderson, 2008). HC treatment resulted in increased photosynthetic carbon fixation rates of *P. tricornutum* with up-regulation of expression levels for most genes involved in carbon-fixation pathways. Moreover, the PSII light energy conversion efficiency (F_v/F_m) of *P. tricornutum* grown under HC conditions was also higher, which would serve to continuously provide reductant and ATP for downstream CO₂ assimilation. Overall, these results suggested that more organic carbon was generated in *P. tricornutum* cells in the HC conditions, which could also further enhance their growth. An increase in the growth of algal cells under HC conditions was observed (2.4%), although increased photosynthetic carbon fixation in this treatment was more pronounced (13.5%). These contrasting results may indicate that the fixed carbon could also have been released as EPS to meet the demand for basic somatic growth.

Elevated environmental CO₂ concentrations may facilitate carbon fixation by phytoplankton, as suggested by several studies of algal cells (Wu et al., 2010; Shi et al., 2019), including the present study. Thus, it is generally expected that increased seawater CO₂ concentrations will enhance marine primary productivity. However, these results also suggest that a fraction of this fixed carbon could be released into seawater via EPS, thereby introducing further uncertainty to the carbon-based response of diatoms to increased ocean CO₂ concentrations. EPS release rival that of other types of DOM that would be released in terms of carbon budgets is a question worthy exploring. In addition, the interactive effects of seawater pH and other environmental factors introduce further uncertainty in these predictions (Gao et al., 2012; Riebesell and Gattuso, 2014). Thus, the effects of EPS over-production on oceanic primary productivity and the biogeochemical cycling of carbon in marine ecosystems requires further investigation.

Nucleotide Diphosphate (NDP)-Sugar Activation and Accelerated Glycosylation Might Be Responsible for HC-Induced EPS Overproduction in *P. tricornutum*

Differential patterns of gene expression alter cellular metabolism and ultimately result in EPS production in diatoms (Aslam et al., 2018). To evaluate the underlying mechanisms for the high-plasticity in carbohydrate and EPS physiology in *P. tricornutum*, genes and divergent alleles related to EPS production were

identified using transcriptomic profiling. A total of 74.0% of these genes had up-regulated expression profiles under HC conditions. In addition, the expression patterns were correlated with physiological and biochemical properties of the cells under HC conditions (RDA analysis, **Figure 5B**).

Two potential responses of *P. tricornutum* EPS metabolism to elevated $p\text{CO}_2$ were identified that could explain the over-release of EPS. First, the pathway of NDP-sugar synthesis and metabolism is a key step in EPS production and one of the substrates for nucleotide acid sugar synthesis is glucose, which is produced during photosynthesis (**Figure 6**, yellow frame). Most of the genes involved in the synthesis and metabolism of glucose and nucleotide sugars were up-regulated in the HC treatment cells. Glucose can be used to generate ATP (i.e., through glycolysis, oxidative phosphorylation, and the TCA cycle) and storage compounds like chrysolaminarin, and are also converted to other sugars and derivatives (Kroth et al., 2008). In particular, glucose is converted to UDP-glucose by glucokinase, glucose phosphate mutase (PGM), and UDP-*N*-acetylglucosamine diphosphorylase. UDP-glucose is a nucleotide sugar that can then be converted to UDP-galactose, and also converted to UDP-glucuronic acid, and further modified to UDP-xylose and UDP-arabinose. Importantly, UDP-glucose conversion is the only source of UDP-xylose and UDP-rhamnose, with no genes encoding arabinose kinase that could convert the monosaccharide to UDP-xylose and UDP-rhamnose being identified in the *P. tricornutum* genome. Nevertheless, rhamnose and xylose content is suboptimal for EPS production compared to glucose (**Figure 2C**). UDP-glucose 6-dehydrogenase promotes the conversion of UDP-glucose to UDP-glucuronic acid and its expression levels were elevated in the HC treatment cells, which could explain the increased uronic acid content in the EPS of those cells. Glucose-1-phosphate can enter the polyketide sugar unit biosynthesis pathway (ko00523) as a substrate, where it is converted to a dTDP-sugar and enters other metabolic pathways. A gene encoding fructokinase that converts fructose to fructose-6-phosphate was not observed in *P. tricornutum*, although fructokinase orthologs have been reported in the diatoms *Thalassiosira* and *Fragilariopsis*. Thus, this reaction may be catalyzed by an unidentified enzyme. An alternative possibility is that fructose-6-phosphate may derive from glycolysis or gluconeogenesis in *P. tricornutum* since genes in the glycolysis/gluconeogenesis pathways (ko00010) that convert 3-phosphoglycerate to fructose-6-phosphate, were significantly up-regulated in cells within the HC treatment. Fructose-6-phosphate can be further converted to glucosamine-6-phosphate, mannose-6-phosphate, or glucose-6-phosphate. Indeed, the expression levels of genes encoding glutamine-fructose-6-phosphate transaminase, mannose-6-phosphate isomerase, and glucose-6-phosphate isomerase, which are all responsible for these reactions were up-regulated in cells of the HC treatment. Glucosamine-6-phosphate is converted to chitosan by phosphor-acetylglucosamine mutase, UDP-*N*-acetylglucosamine, and chitin synthase. However, the expression levels of the encoded chitin synthase gene and the gene encoding UDP-*N*-acetylglucosamine were not down-regulated in HC treatment cells, suggesting that fructose-6-phosphate

may be more likely converted to mannose-6-phosphate or glucose-6-phosphate, thereby leading to NDP-sugar production.

A second mechanism explaining the EPS response by *P. tricornutum* to high $p\text{CO}_2$ levels could be that most genes encoding GTs and ABC transporter systems in the ER or Golgi bodies were up-regulated, which altered the polymerization steps of EPS synthesis (**Figure 6**, orange and purple frame). The Golgi apparatus is the major site of glycosylation reactions. In contrast, the NDP-sugar substrates of Golgi-associated glycosyltransferases are synthesized in the cytoplasm (Tiwari et al., 2016). Most genes encoding GTs were up-regulated, and increased expression of some ABC transporters indicate potentially increased activity in the Golgi apparatus leading to EPS secretion. These EPS then undergo further self-assembly in external environments and form cell frustule coatings, adhesive structures, or are used for motility (Wetherbee et al., 1998; Willis et al., 2015). The above two mechanistic responses were also observed as responses of *F. cylindrus* to extreme sea ice habitats (Aslam et al., 2018). However, the types of NDP-sugars involved were uniformly the same. For example, besides common NDP-sugars (e.g., GDP-Man, GDP-Fuc, UDP-GlcA, UDP-Glc, UDP-Gal, and UDP-GlcA), the gene encoding the enzymes involved in UDP-Xyl and UDP-Ara were also differentially expressed in response to HC condition. Thus, these combined results suggest that these metabolic pathways are likely common features of EPS production by diatom taxa in response to environmental signals, but some difference of local subdivision suggested these responses were closely related to algal species and environmental factors.

In addition to the above two mechanistic responses to environmental change, the results presented here improve our understanding of NDP-sugar transporters (NSTs) that are important for NDP-sugar interconversions (**Figure 6**, purple frame). An important function of NSTs is to transport NDP-sugars from the site of synthesis in the cytosol, across the membrane into the Golgi apparatus, and then supply substrates for GTs to synthesize polysaccharides and glycoproteins (Gerardy-Schahn et al., 2001; Zhang et al., 2011). NSTs were originally described in animal cells but are present throughout all eukaryotes that have been evaluated (Hirschberg et al., 1998). Changes in NST expression can affect glycoprotein biosynthesis and then indirectly affect polysaccharide levels on coat surfaces (Hadley et al., 2014). A total of eight genes encoding putative NSTs were identified in the *P. tricornutum* genome, of which seven were significantly up-regulated, implicating their role in EPS over-production in response to elevated $p\text{CO}_2$ levels.

CONCLUSION

In summary, our study showed that elevated $p\text{CO}_2$ levels facilitate the increased release of EPS from *P. tricornutum* diatom cells and alter their chemical compositions. These data suggest that EPS release is likely due to carbon fixation outpacing carbon needed for growth, leading to the over-synthesis of carbon-rich storage products. NDP-sugar activation and accelerated glycosylation are two possible mechanisms that could explain the increased

EPS production in response to environmental changes. Further, up-regulation of NDP-sugar transporters could also play an important role in EPS over-production in response to elevated *p*CO₂ levels. This is the first report to show that both molecular and metabolic plasticity is required of *P. tricornutum* to cope with elevated *p*CO₂ levels. These results provide a more resolved model for the production of EPS by diatoms and contribute to a better understanding of the response of EPS metabolism to environmental signals, and especially increased *p*CO₂ levels.

DATA AVAILABILITY STATEMENT

The RNA-seq data were deposited in the ArrayExpress database (www.ebi.ac.uk/arrayexpress) under accession number E-MTAB-8351.

AUTHOR CONTRIBUTIONS

XXZ were responsible for the conception and design of this research. WZ, YY, and XZ were responsible for data collection and collation. WZ responsible for analysis, interpretation,

REFERENCES

- Abdullahi, A. S., Underwood, G. J. C., and Gretz, M. R. (2006). Extracellular matrix assembly in diatoms (bacillariophyceae). v. environmental effects on polysaccharide synthesis in the model diatom, *Phaeodactylum tricornutum* 1. *J. Phycol.* 42, 363–378. doi: 10.1111/j.1529-8817.2006.00193.x
- Ai, X.-X., Liang, J.-R., Gao, Y.-H., Lo, S. C.-L., Lee, F. W.-F., Chen, C.-P., et al. (2015). MALDI-TOF MS analysis of the extracellular polysaccharides released by the diatom *Thalassiosira pseudonana* under various nutrient conditions. *J. Appl. Phycol.* 27, 673–684. doi: 10.1007/s10811-014-0360-0
- Anders, S., and Huber, W. (2012). *Differential Expression of RNA-Seq Data at the Gene Level—the DESeq Package*. Heidelberg: European Molecular Biology Laboratory (EMBL).
- Anders, S., Pyl, P. T., and Huber, W. (2015). HTSeq—a Python framework to work with high-throughput sequencing data. *Bioinformatics* 31, 166–169. doi: 10.1093/bioinformatics/btu638
- Aslam, S. N., Cresswell—Maynard, T., Thomas, D. N., and Underwood, G. J. C. (2012). Production and characterization of the intra—and extracellular carbohydrates and polymeric substances (EPS) of three sea—ice diatom species, and evidence for a cryoprotective role for EPS. *J. Phycol.* 48, 1494–1509. doi: 10.1111/jpy.12004
- Aslam, S. N., Strauss, J., Thomas, D. N., Mock, T., and Gjc, U. (2018). Identifying metabolic pathways for production of extracellular polymeric substances by the diatom *Fragilariopsis cylindrus* inhabiting sea ice. *ISME J.* 12, 1237–1251. doi: 10.1038/s41396-017-0039-z
- Berman-Frank, I., and Dubinsky, Z. (1999). Balanced growth in aquatic plants: myth or reality? Phytoplankton use the imbalance between carbon assimilation and biomass production to their strategic advantage. *Bioscience* 49, 29–37. doi: 10.1525/bisi.1999.49.1.29
- Bolger, A. M., Lohse, M., and Usadel, B. (2014). Trimmomatic: a flexible trimmer for Illumina sequence data. *Bioinformatics* 30, 2114–2120. doi: 10.1093/bioinformatics/btu170
- Calazans, G. M. T., Lima, R. C., de França, F. P., and Lopes, C. E. (2000). Molecular weight and antitumor activity of *Zymomonas mobilis* levans. *Int. J. Biol. Macromol.* 27, 245–247. doi: 10.1016/s0141-8130(00)00125-2
- Czaczyk, K., and Myszyka, K. (2007). Biosynthesis of extracellular polymeric substances (EPS) and its role in microbial biofilm formation. *Pol. J. Environ. Stud.* 16, 799–806. r

and manuscript content. The approval of XT was obtained prior to article submission and provided financial support for this research.

FUNDING

This work was financially supported by the Natural Science Foundation of the Shandong Province (ZR2017BD020) and the National Natural Science Foundation of China (41706123).

ACKNOWLEDGMENTS

The authors thank the members of the lab for their kind help. They also thank Accdon for editing for English language.

SUPPLEMENTARY MATERIAL

The Supplementary Material for this article can be found online at: <https://www.frontiersin.org/articles/10.3389/fmicb.2020.00339/full#supplementary-material>

- de Brouwer, J. F., Wolfstein, K., Ruddy, G. K., Jones, T. E., and Stal, L. J. (2005). Biogenic stabilization of intertidal sediments: the importance of extracellular polymeric substances produced by benthic diatoms. *Microb. Ecol.* 49, 501–512. doi: 10.1007/s00248-004-0020-z
- de Brouwer, J. F. C., Ruddy, G. K., Jones, T. E. R., and Stal, L. J. (2002). Sorption of EPS to sediment particles and the effect on the rheology of sediment slurries. *Biogeochemistry* 61, 57–71. doi: 10.1016/j.watres.2009.06.031
- Decho, A. W., and Gutierrez, T. (2017). Microbial extracellular polymeric substances (epss) in ocean systems. *Front. Microbiol.* 8:922. doi: 10.3389/fmicb.2017.00922
- Decho, A. W., and Luoma, S. N. (1994). Humic and fulvic acids: sink or source in the availability of metals to the marine bivalves *Macoma balthica* and *Potamocorbula amurensis*? *Mar. Ecol. Prog. Ser.* 108:133. doi: 10.3354/meps108133
- Deming, J. W. (2010). Sea ice bacteria and viruses. *Sea Ice* 2, 247–282. doi: 10.1002/9781444317145.ch7
- Doney, S. C., Fabry, V. J., Feely, R. A., and Kleypas, J. A. (2009). Ocean acidification: the other CO₂ problem. *Annu. Rev. Mar. Sci.* 1, 169–192. doi: 10.1146/annurev.marine.010908.163834
- Donot, F., Fontana, A., Baccou, J. C., and Schorr-Galindo, S. (2012). Microbial exopolysaccharides: main examples of synthesis, excretion, genetics and extraction. *Carbohydr. Polym.* 87, 951–962. doi: 10.1016/j.carbpol.2011.08.083
- Fu, F. X., Tatters, A. O., and Hutchins, D. A. (2012). Global change and the future of harmful algal blooms in the ocean. *Mar. Ecol. Prog. Ser.* 470, 207–233. doi: 10.3354/meps10047
- Gao, K., and Campbell, D. A. (2014). Photophysiological responses of marine diatoms to elevated CO₂ and decreased pH: a review. *Funct. Plant. Biol.* 41, 449–459. doi: 10.1071/fp13247
- Gao, K., Helbling, E. W., Häder, D.-P., and Hutchins, D. A. (2012). Responses of marine primary producers to interactions between ocean acidification, solar radiation, and warming. *Mar. Ecol. Prog. Ser.* 470, 167–189. doi: 10.3354/meps10043
- Gerardy-Schahn, R., Oelmann, S., and Bakker, H. (2001). Nucleotide sugar transporters: biological and functional aspects. *Biochimie* 83, 775–782. doi: 10.1016/s0300-9084(01)01322-0
- Gu, Z., Eils, R., and Schlesner, M. (2016). Complex heatmaps reveal patterns and correlations in multidimensional genomic data. *Bioinformatics* 32, 2847–2849. doi: 10.1093/bioinformatics/btw313

- Gügi, B., le Costaouec, T., Burel, C., Lerouge, P., Helbert, W., and Bardor, M. (2015). Diatom-specific oligosaccharide and polysaccharide structures help to unravel biosynthetic capabilities in diatoms. *Mar. Drugs* 13, 5993–6018. doi: 10.3390/md13095993
- Guillard, R. R. L. (1975). "Culture of phytoplankton for feeding marine invertebrates," in *Culture of Marine Invertebrate Animals*, eds W. L. Smith, and M. H. Chanley, (Boston, MA: Springer), 29–60. doi: 10.1007/978-1-4615-8714-9_3
- Hadley, B., Maggioni, A., Ashikov, A., Day, C. J., Haselhorst, T., and Tiralongo, J. (2014). Structure and function of nucleotide sugar transporters: current progress. *Comput. Struct. Biotechnol. J.* 10, 23–32. doi: 10.1016/j.csbj.2014.05.003
- Hessen, D. O., and Anderson, T. R. (2008). Excess carbon in aquatic organisms and ecosystems: physiological, ecological, and evolutionary implications. *Limnol. Oceanogr.* 53, 1685–1696. doi: 10.4319/lo.2008.53.4.1685
- Hirschberg, K., Miller, C. M., Ellenberg, J., Presley, J. F., Siggia, E. D., Phair, R. D., et al. (1998). Kinetic analysis of secretory protein traffic and characterization of Golgi to plasma membrane transport intermediates in living cells. *J. Cell Biol.* 143, 1485–1503. doi: 10.1083/jcb.143.6.1485
- Hong, H., Shen, R., Zhang, F., Wen, Z., Chang, S., Lin, W., et al. (2017). The complex effects of ocean acidification on the prominent N₂-fixing cyanobacterium *Trichodesmium*. *Science* 356, 527–531. doi: 10.1126/science.aao428
- Hutchins, D. A., Fu, F.-X., Zhang, Y., Warner, M. E., Feng, Y., Portune, K., et al. (2007). CO₂ control of *Trichodesmium* N₂ fixation, photosynthesis, growth rates, and elemental ratios: implications for past, present, and future ocean biogeochemistry. *Limnol. Oceanogr.* 52, 1293–1304. doi: 10.4319/lo.2007.52.4.1293
- Jin, P., Wang, T., Liu, N., Dupont, S., Beardall, J., Boyd, P. W., et al. (2015). Ocean acidification increases the accumulation of toxic phenolic compounds across trophic levels. *Nat. Commun.* 6:8714. doi: 10.1038/ncomms9714
- Kaplan, D. (2013). Absorption and adsorption of heavy metals by microalgae. Handbook of microalgal culture. *Appl. Phycol. Biotechnol.* 2, 602–611. doi: 10.1002/9780470995280.ch26
- Kim, D., Langmead, B., and Salzberg, S. L. (2015). HISAT: a fast spliced aligner with low memory requirements. *Nat. Methods* 12, 357–360. doi: 10.1038/nmeth.3317
- Kooistra, W. H., De Stefano, M., Mann, D. G., and Medlin, K. (2003). "The Phylogeny of the Diatoms," in *Silicon Biomineralization. Progress in Molecular and Subcellular Biology*, Vol. 33, ed. W. E. G. Müller, (Berlin: Springer).
- Kroth, P. G., Chiovitti, A., Gruber, A., Martinjezequel, V., Mock, T., Parker, M. S., et al. (2008). A model for carbohydrate metabolism in the diatom *Phaeodactylum tricornutum* deduced from comparative whole genome analysis. *PLoS One* 3:e1426. doi: 10.1371/journal.pone.0001426
- Macías-Sánchez, M. D., Mantell, C., Rodríguez, M., Ossa, E. M. D., la, Lubián, L. M., and Montero, O. (2007). Supercritical fluid extraction of carotenoids and chlorophyll a from *Synechococcus* sp. *J. Supercrit. Fluids* 39, 323–329. doi: 10.1016/j.supflu.2006.03.008
- Magaletti, E., Urbani, R., Sist, P., Ferrari, C. R., and Cicero, A. M. (2004). Abundance and chemical characterization of extracellular carbohydrates released by the marine diatom *Cylindrotheca fusiformis* under N- and P-limitation. *European J. Phycol.* 39, 133–142. doi: 10.1080/0967026042000202118
- Mcconville, M. J., Mitchell, C., and Wetherbee, R. (1985). Patterns of carbon assimilation in a microalgal community from annual sea ice, east Antarctica. *Polar. Biol.* 4, 135–141. doi: 10.1007/bf00263876
- Middelburg, J. J., Barranguet, C., Boschker, H. T. S., Herman, P. M. J., Moens, T., and Heip, C. H. R. (2000). The fate of intertidal microphytobenthos carbon: an in situ ¹³C-labeling study. *Limnol. Oceanogr.* 45, 1224–1234. doi: 10.4319/lo.2000.45.6.1224
- Millero, F. J., Huang, F., Williams, N., Waters, J., and Woosley, R. (2009). The effect of composition on the density of South Pacific Ocean waters. *Mar. Chem.* 114, 56–62. doi: 10.1016/j.marchem.2009.04.001
- Mishra, A., and Jha, B. (2009). Isolation and characterization of extracellular polymeric substances from micro-algae *Dunaliella salina* under salt stress. *Bioresour. Technol.* 100, 3382–3386. doi: 10.1016/j.biortech.2009.02.006
- Mitchell, A. L., Attwood, T. K., Babbitt, P. C., Blum, M., Bork, P., Bridge, A., et al. (2018). InterPro in 2019: improving coverage, classification and access to protein sequence annotations. *Nucleic Acids Res.* 47, D351–D360. doi: 10.1093/nar/gky1100
- Nielsen, H. (2017). Predicting secretory proteins with SignalP. *Methods Mol. Biol.* 1611, 59–73. doi: 10.1007/978-1-4939-7015-5_6
- Oksanen, J., Blanchet, F. G., Kindt, R., Legendre, P., O'hara, R. B., Simpson, G. L., et al. (2003). VEGAN, a package of R functions for community ecology. *J. Veg. Sci.* 14, 927–930. doi: 10.1111/j.1654-1103.2003.tb02228.x
- Porra, R. J., Thompson, W. A., and Kriedemann, P. E. (1989). Determination of accurate extinction coefficients and simultaneous equations for assaying chlorophylls a and b extracted with four different solvents: verification of the concentration of chlorophyll standards by atomic absorption spectroscopy. *Biochim. Biophys. Acta Bioenerg.* 975, 384–394. doi: 10.1016/S0005-2728(89)80347-0
- Riebesell, U., and Gattuso, J.-P. (2014). Lessons learned from ocean acidification research. *Nat. Clim. Chang.* 5, 12–14. doi: 10.1038/nclimate2456
- Scala, S., Carels, N., Falcioratore, A., Chiusano, M. L., and Bowler, C. (2002). Genome properties of the diatom *Phaeodactylum tricornutum*. *Plant Physiol.* 129, 993–1002. doi: 10.1104/pp.010713
- Shi, D., Hong, H., Su, X., Liao, L., Chang, S., and Lin, W. (2019). The physiological response of marine diatoms to ocean acidification: differential roles of seawater pCO₂ and pH. *J. Phycol.* 55, 521–533. doi: 10.1111/jpy.12855
- Siaut, M., Heijde, M., Mangogna, M., Montsant, A., Coesel, S., Allen, A., et al. (2007). Molecular toolbox for studying diatom biology in *Phaeodactylum tricornutum*. *Gene* 406, 23–35. doi: 10.1016/j.gene.2007.05.022
- Simon, M., Grossart, H.-P., Schweitzer, B., and Ploug, H. (2002). Microbial ecology of organic aggregates in aquatic ecosystems. *Aquat. Microb. Ecol.* 28, 175–211. doi: 10.3354/ame028175
- Song, W., Zhao, C., Mu, S., Pan, X., Zhang, D., Al-Misned, F. A., et al. (2015). Effects of irradiation and pH on fluorescence properties and flocculation of extracellular polymeric substances from the cyanobacterium *Chroococcus minutus*. *Colloids Surf. B* 128, 115–118. doi: 10.1016/j.colsurfb.2015.02.017
- Sonnenschein, E. C., Gärdes, A., Seebah, S., Torres-Monroy, I., Grossart, H.-P., and Ullrich, M. S. (2011). Development of a genetic system for *Marinobacter adhaerens* HP15 involved in marine aggregate formation by interacting with diatom cells. *J. Microbiol. Methods* 87, 176–183. doi: 10.1016/j.mimet.2011.08.008
- Steele, D. J., Franklin, D. J., and Underwood, G. J. C. (2014). Protection of cells from salinity stress by extracellular polymeric substances in diatom biofilms. *Biofouling* 30, 987–998. doi: 10.1080/08927014.2014.960859
- Sutherland, I. W. (1999). "Biofilm Exopolysaccharides," in *Microbial Extracellular Polymeric Substances*, eds J. Wingender, T. R. Neu, and H. C. Flemming, (Berlin: Springer). doi: 10.1007/978-3-642-60147-7_4
- Taylor, J. D., McKew, B. A., Kuhl, A., McGenity, T. J., and Underwood, G. J. C. (2013). Microphytobenthic extracellular polymeric substances (EPS) in intertidal sediments fuel both generalist and specialist EPS-degrading bacteria. *Limnol. Oceanogr.* 58, 1463–1480.
- Tiwari, P., Sangwan, R. S., and Sangwan, N. S. (2016). Plant secondary metabolism linked glycosyltransferases: an update on expanding knowledge and scopes. *Biotechnol. Adv.* 34, 714–739. doi: 10.1016/j.biotechadv.2016.03.006
- Trapnell, C., Williams, B. A., Pertea, G., Mortazavi, A., Kwan, G., van Baren, M. J., et al. (2010). Transcript assembly and quantification by RNA-Seq reveals unannotated transcripts and isoform switching during cell differentiation. *Nat. Biotechnol.* 28, 511–515. doi: 10.1038/nbt.1621
- Underwood, G. J. C., Aslam, S. N., Michel, C., Niemi, A., Norman, L., Meiners, K. M., et al. (2013). Broad-scale predictability of carbohydrates and exopolymers in Antarctic and Arctic sea ice. *Proc. Natl. Acad. Sci. U.S.A.* 110, 15734–15739. doi: 10.1073/pnas.1302870110
- Underwood, G. J. C., Boulcott, M., Raines, C. A., and Waldron, K. (2004). Environmental effects on exopolymer production by marine benthic diatoms: dynamics, changes in composition, and pathways of production I. *J. Phycol.* 40, 293–304. doi: 10.1111/j.1529-8817.2004.03076.x

- Underwood, G. J. C., and Paterson, D. M. (2003). The importance of extracellular carbohydrate production by marine epipelagic diatoms. *Adv. Bot. Res.* 40, 183–240. doi: 10.1016/S0065-2296(05)40005-1
- Wetherbee, R., Lind, J. L., Burke, J., and Quatrano, R. S. (1998). Minireview—the first kiss: establishment and control of initial adhesion by raphid diatoms. *J. Phycol.* 34, 9–15. doi: 10.1046/j.1529-8817.1998.340009.x
- Wickham, H. (2016). *ggplot2: Elegant Graphics for Data Analysis*. Berlin: Springer.
- Willis, A., Easonhubbard, M., Hodson, O., Maheswari, U., Bowler, C., and Wetherbee, R. (2015). Adhesion molecules from the diatom *Phaeodactylum tricornutum* (Bacillariophyceae): genomic identification by amino-acid profiling and in vivo analysis. *J. Phycol.* 50, 837–849. doi: 10.1111/jpy.12214
- Wu, Y., Gao, K., and Riebesell, U. (2010). CO₂-induced seawater acidification affects physiological performance of the marine diatom *Phaeodactylum tricornutum*. *Biogeosciences* 7, 2915–2923. doi: 10.5194/bg-7-2915-2010
- Zhang, B., Liu, X., Qian, Q., Liu, L., Dong, G., Xiong, G., et al. (2011). Golgi nucleotide sugar transporter modulates cell wall biosynthesis and plant growth in rice. *Proc. Natl. Acad. Sci. U.S.A.* 108, 5110–5115. doi: 10.1073/pnas.1016144108

Conflict of Interest: The authors declare that the research was conducted in the absence of any commercial or financial relationships that could be construed as a potential conflict of interest.

Copyright © 2020 Zhang, Tang, Yang, Zhang and Zhang. This is an open-access article distributed under the terms of the Creative Commons Attribution License (CC BY). The use, distribution or reproduction in other forums is permitted, provided the original author(s) and the copyright owner(s) are credited and that the original publication in this journal is cited, in accordance with accepted academic practice. No use, distribution or reproduction is permitted which does not comply with these terms.